

**N94-11399****A HIGH SPECIFIC POWER SOLAR ARRAY FOR LOW TO MID-POWER SPACECRAFT**

P. Alan Jones, Stephen F. White and T. Jeffery Harvey  
*AEC-Able Engineering Company, Inc.*  
*Goleta, California 93117*

Brian S. Smith  
*Spectrolab, Inc.*  
*Sylmar, California 91342-5373*

---

UltraFlex is the generic term for a solar array system which delivers on-orbit power in the 400 to 6,000 watt per wing sizes with end-of-life specific power performance ranging to 150 watts-per-kilogram. Such performance is accomplished with off-the-shelf solar cells and state-of-the-art materials and processes.

Much of the recent work in photovoltaics is centered on advanced solar cell development. Successful as such work has been, no integrated solar array system has emerged which meets NASA's stated goals of "increasing the end-of-life performance of space solar cells and arrays while minimizing their mass and cost." Here we address this issue; namely, is there an array design that satisfies the usual requirements for space-rated hardware and that is inherently reliable, inexpensive, easily manufactured and simple, which can be used with both advanced cells currently in development and with inexpensive silicon cells? The answer is yes.

The UltraFlex array described below incorporates use of a blanket substrate which is thermally compatible with silicon and other materials typical of advanced multi-junction devices. The blanket materials are intrinsically insensitive to atomic oxygen degradation, are space rated, and are compatible with standard cell bonding processes. The deployment mechanism is simple and reliable and the structure is inherently stiff (high natural frequency). Mechanical vibration modes are also readily damped.

The basic design is presented as well as supporting analysis and development tests.

---

**INTRODUCTION**

To obtain program funding in today's political-economic environment it is a practical necessity for spacecraft programs to either maximize return through increased operational payloads or reduce launch costs with a less massive spacecraft. Dual motivations exist for reducing spacecraft mass: The increasing costs for existing launch systems and the introduction of new low-cost, low-payload launch vehicles (Pegasus, Taurus, Connestoga, etc.). A low-cost, lightweight spacecraft power source can contribute towards this end.

The preferred power source for most spacecraft launched today is a solar cell array [1]. Solar cell arrays provide clean, long-term spacecraft power at a reasonable cost. Great benefits to the spacecraft mission can be realized with any significant increase in solar array specific power. The resultant reduced solar array mass allows for the allocation of more mass to other spacecraft features. These can be additional communication transponders or scientific instruments, or additional station-keeping fuel to allow longer on-station life. In addition, overall spacecraft mass may be reduced, rather than reallocated, to allow for the use of a smaller, more economical launch vehicle or, perhaps, a more profitable mission orbit. However this performance dividend is actually realized, increased solar array specific power can provide large cost/performance benefits to the spacecraft designer.

While increased array specific power is a very attractive goal, its benefits must not be mitigated by an increase in solar array subsystem cost. Recent solar cell technological advances have the potential to improve specific power however, the issues of environmental durability, large-scale manufacturability, and cost cloud their potential. Spacecraft designers in the near future must therefore rely on well established solar cell technologies to meet the coupled goal of increased specific power at a reasonable cost.

Such a solar array system which is currently under development by AEC-Able Engineering in collaboration with Spectrolab. Present development progress to-date indicates an end-of-life (EOL) specific power of 125 W/kg for a 634-watt 7-year low-earth-orbit (LEO) mission with silicon cells. A larger 3986 watt version produces 140 W/kg. Gallium-cell-based UltraFlex arrays will produce on the order of 153 W/kg at the 3131 watt scale. These values greatly exceed typical rigid array specific powers in the range of 35 to 40 W/kg. Conventional silicon or gallium solar cells coupled with a unique mechanical/structural system enable the UltraFlex solar array to provide superior performance with today's established technologies.

### BACKGROUND

The specific power performance data for several rigid and flexible solar arrays have been compiled in Figure 1. Since the various arrays are designed to varied requirements and environments the data in Figure 1 should be interpreted as a general historic overview rather than as a point-to-point comparison. Considerable effort, by various authors, has been extended on estimating the break-point in total array power below which a rigid array is more advantageous versus a flexible array. Total array power values from 4 to 10 kW have been offered [2] as break points above which rigid arrays are less desirable due to cost, reliability, and performance.

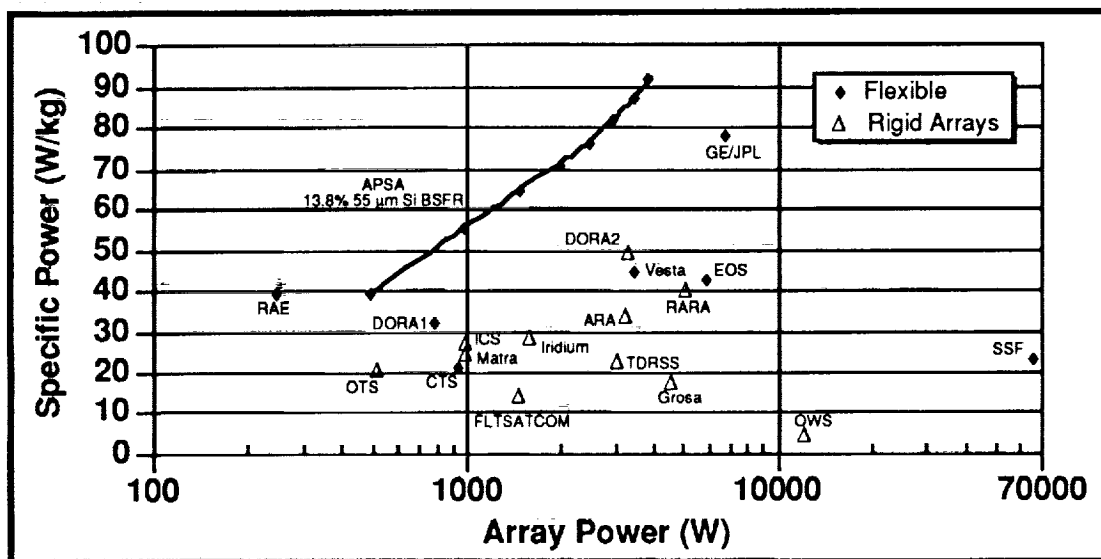


Figure 1  
Solar Array Specific Power Versus Array Power

The performance break-point can be illustrated by the JPL-developed Advanced Photovoltaic Solar Array (APSA) data shown above. While the APSA system produces 92.5 W/kg at 3.9 kW, mass efficiency drops to 40 W/kg at 0.5 kW [3]. This drop is due to the non-linear mass scaling of its structural components. Most notable are the deployment mast system and the blanket containment structures. The curve of APSA specific power versus power data crosses the typical rigid array specific power (40 W/kg) at approximately 1/2 kW. The performance break-point will occur at higher power levels for less-optimized array designs (EOS and SSF).

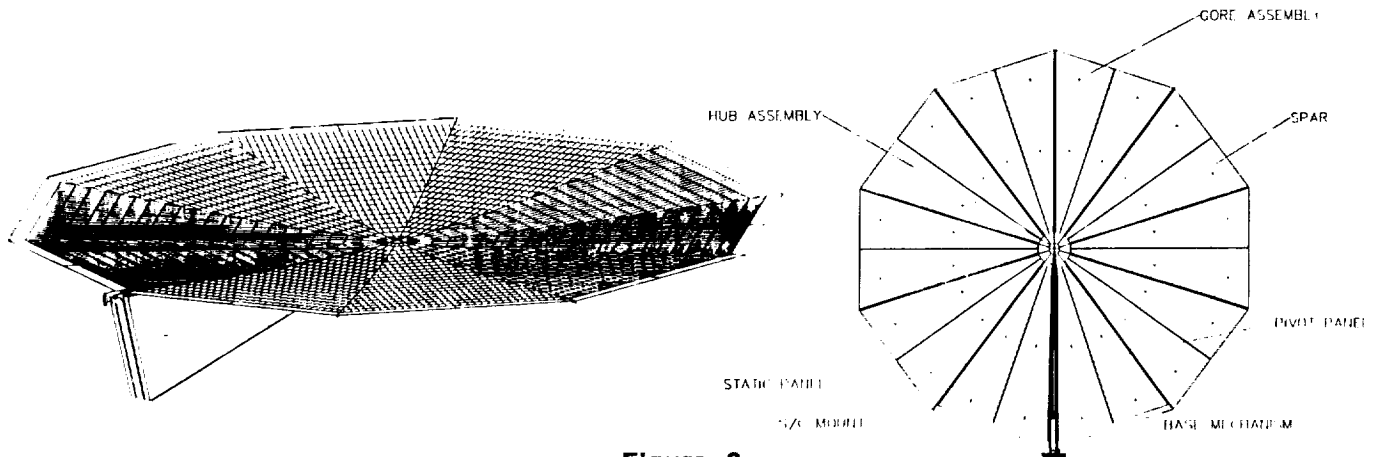
The APSA program was very successful in meeting its general goal: the development of a high performance photovoltaic solar array. The program laid a solid foundation of work in the areas of ultra-thin solar cell usage, lightweight substrates, and optimized structures. The APSA program currently reports the highest specific array power of any tested solar array. It is evident, from the data in Figure 1, that very high specific power solar arrays (150 W/kg) in the 0.5 to 2.0 kW power range do not exist in any deployable form. This is the performance niche that UltraFlex targets.

## DESIGN CONFIGURATION

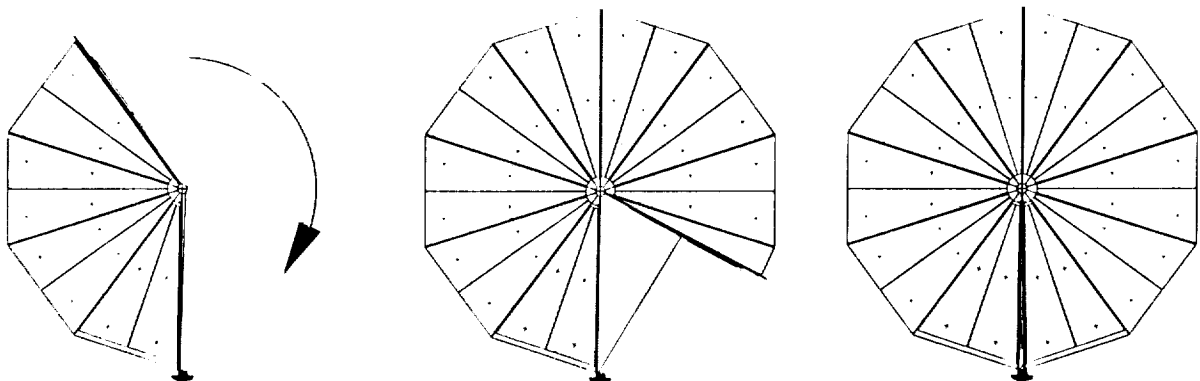
An initial study indicated that only flexible substrate solar arrays could produce the desired 150 W/kg specific power performance at low power levels. ABLE initiated a design effort to produce a solar array that satisfied the structural requirements displayed in Table 1 and delivered superior specific power performance.

Table 1 STRUCTURAL REQUIREMENTS	
Stowed First Mode	30 Hz, Minimum
Deployed First Mode	0.1 Hz, Minimum
Stowed Maximum G's	25 g normal, 30 g lateral
Deployed Maximum G's	0.1 g (all axes)
Launch Acoustic Vibration	146 dB Overall

The result is the UltraFlex solar array\*, shown isometrically and in plan view in Figure 2. It is a departure from the standard rectangular shape typically seen in rigid or flexible arrays. The UltraFlex deploys a flexible cell blanket into a multisided polygon using a fan-like deployment, shown schematically in Figure 3. The individual gore assemblies have flexure hingelines at the gore centerline. During deployment the system flexes into a tensioned, complex paraboloid. The pre-stressed shape acts to stiffen the deployed structure enabling reasonably high natural frequencies. A mockup was constructed which depicts the deployed shape (Figure 4).



**Figure 2**  
**UltraFlex Deployed Configuration**



**Figure 3**  
**UltraFlex Deployment Sequence**

\* Patent Pending

Prior to deployment the array is sandwiched between two structural panels which, through the use of a compressed polyimide foam, maintain sufficient areal pressure on the solar cells to survive launch vibratory loads. This established approach is the baseline on the APSA and Space Station solar array systems [3,4]. The two structural panels (denoted pivot panel and static panel) are hinged together at one end by a hub mechanism.

Two pyrotechnically released tiedown mechanisms are used to secure the system to the spacecraft for launch. In addition to the two active launch restraints mentioned, three other passive cup-cone assemblies complete the launch restraint system. After launch tiedown release, deployment is accomplished by the rotation of the pivot panel about the central hub away from the static panel. Deployment torque is provided by a DC motor system. The pivot panel rotates a full 360° pulling and tensioning the hinged-together blanket subassemblies into their deployed configuration. After this rotation the pivot panel is latched to the static panel with a passive latch mechanism.

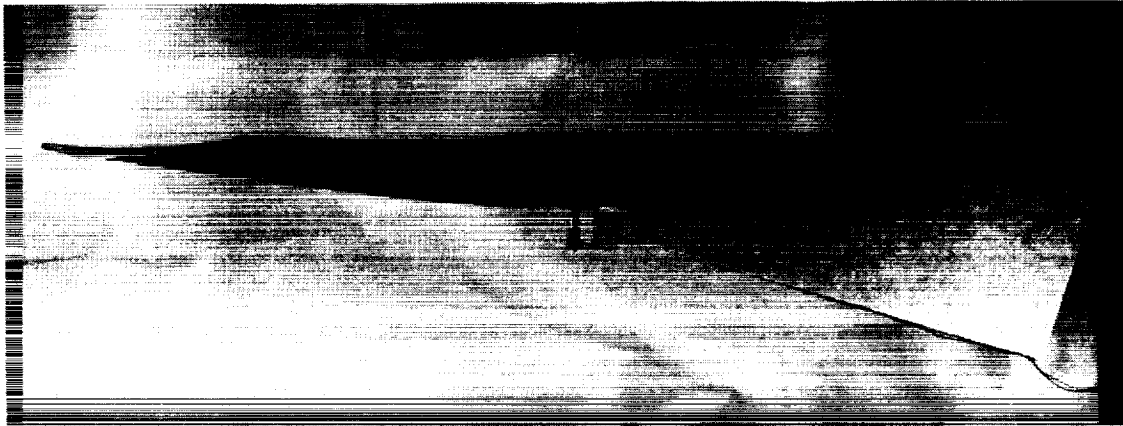


**Figure 4**  
**UltraFlex Mockup**

### **Substrate**

Though Kapton has had excellent flight history, its use as a blanket substrate is marred by two problems: it degrades in the presence of atomic oxygen and it readily tears once a flaw is introduced. Due to these concerns ABLE developed a new substrate for the UltraFlex array.

First, the material should be 100% compatible with the space environment, both low earth and geostationary. Secondly, the material should lend itself to established cell laydown and attachment practices to minimize the extent and cost of requalification. Lastly, the material should have good dielectric, low mass, and low cost characteristics. During the initial UltraFlex conceptualization a re-evaluation of flexible blanket material options offered some interesting possibilities. To satisfy the above requirements a flexible composite substrate\* has been developed which combines an inorganic open-weave fabric with an inorganic binder resin. The inorganic nature of both materials should preclude their corrosion in the atomic oxygen environment.

Solar cell to substrate compatibility is, to a large measure, dictated by their relative coefficients of thermal expansion (CTE). The effective CTE of the UltraFlex substrate is estimated to be  $0.51 \mu\text{in}/\text{in}/^\circ\text{F}$ . The resultant substrate-to-silicon cell CTE mismatch is estimated to be less than  $0.93 \mu\text{in}/\text{in}/^\circ\text{F}$ . For GaAs/Ge solar cells the mismatch is  $2.7 \mu\text{in}/\text{in}/^\circ\text{F}$ . These low CTE mismatch values are desired to assure good thermal cycle capability. By comparison, the CTE mismatch of Kapton H with silicon cells is about  $26.5 \mu\text{in}/\text{in}/^\circ\text{F}$ .

The choice of an open-scrim material was intended to reduce areal mass and provide for good cell heat rejection. The substrate openings, approximately 60%, allow for the direct emission from the rear surface of the solar cell. Typically, the rearside heat loss must first be conducted from the cell through the substrate to finally be emitted from the rearside. Solar cells currently have a low rearside emissivity, on the order of 0.12. Coatings on the cell backside to improve emission have been attempted in the past [1]. If implemented, these coatings will improve UltraFlex performance through reduced cell operating temperature.

---

\* Patent Pending

## Gore Subassembly

The gore subassembly consists of the substrate material, edge spars, solar cells, and a flex-circuit harness section. The subassembly is assembled in its deployed, tensioned shape to assure proper distribution of membrane preload forces. To maintain low recurring costs, a primary substrate requirement was for good compatibility with established solar cell attachment techniques. This has been established through bonding trials at Spectrolab and subsequent thermal cycle testing at ABLE.

The triangular shape of the gore subassembly (Figure 5) unfortunately inhibits efficient cell packing. To maximize packing factor the number of cells per string are reduced one-per-row. Thus, the geometry of the gores are directly linked to the aspect ratio of the solar cell. Since there are only integer choices for array geometry (e.g., 8, 9, or 10 gores per wing) solar cell aspect ratios are limited to discrete values.

Electrical power is collected from the solar cell strings and routed to the base of the deployed wing with a Kapton insulated custom flex circuit. For LEO applications the Kapton is coated an  $\text{SiO}_{1.9-2.0}$  coating. The multi-fingered flex circuit harnesses are bonded to the gore rearsides during the assembly process. The ends of these fingers have redundant bared solder pads for direct interface with the cell circuits. These harnesses lead into a central collection harness which runs around the central hub. This central multi-layer circuit employs specialized pin connectors to interface with the individual gore harnesses.

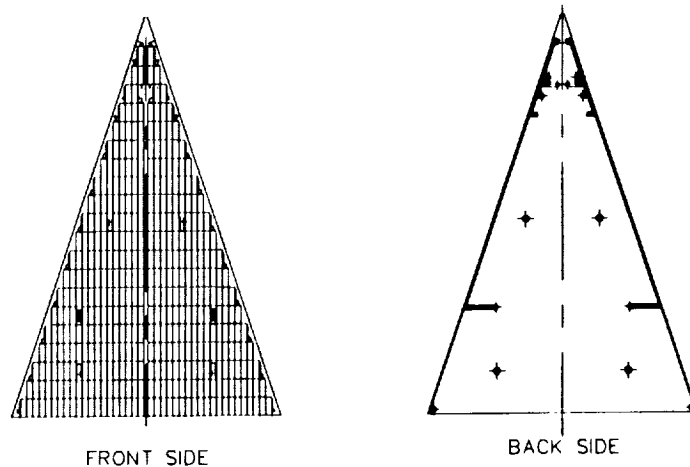


**Figure 5**  
**Gore Subassembly**

## Mechanisms

The UltraFlex obtains its high specific performance by minimizing the quantity and scale of non-power-producing mechanical and structural components required to deploy and support a given area of solar cells. Reliability is also enhanced over typical rigid arrays by the use of a single deployment mechanism and a single latch mechanism rather than two or three hinge/latch mechanisms at each of three to six hingelines. Current reliability estimates indicate a probability of successful deployment to be 0.9975.

The single deployment mechanism consists of an electrically redundant DC brushless motor coupled via a spur geartrain to a lanyard-reel system. Tension is created in the Elgiloy lanyard which, in turn, produces a deploying moment around the center hub. As the system nears full deployment the lanyard serves to pull the pivot panel directly to the latch probe. The latch mechanism, mounted on the static panel, utilizes a spring-loaded male probe to engage the receptacle on the pivot panel. The deploy motor system remains activated until full latching is reached.

---

## DEVELOPMENT TESTS

### Cell-to-Substrate Bond Strength

The main concerns over the compatibility of the material with standard solar cell array bonding techniques lay in whether the silicone adhesive used for bonding the cells would adhere to the substrate and whether the contact area of substrate to cells was sufficient to provide adequate bond strength. In addition, the completed assembly of cells to substrate was to meet stringent low weight goals. A series of tests were performed to address these concerns prior to coupon assembly.

Cell-substrate bonding tests were conducted for two bonding approaches. In the first approach adhesive was applied to the cell surface only. In the second approach adhesive was applied to the substrate only. The bonded samples were then pulled apart to obtain pull strength information. These comparative tests showed that applying adhesive only to the weave gave pull strengths of the order 150 gm while applying adhesive only to the cells gave pull strengths of the order 250 gm. To minimize substrate areal mass and despite its lower strength, the former bonding method was selected.

During additional testing, 0.5 in. wide by 2 in. long strips of the open weave material were bonded to the rearside of solar cells. Control samples of Kapton of the same dimensions were similarly bonded. After curing the adhesive, all samples were pulled. The open weave material had an average over ten samples of 96 gm, while the Kapton control specimens (3) had an average of 176 gm. These values reflected the area of contact of the two materials. The open weave has an approximate bond fill factor of 50%.

### Thermal Cycle Testing

A primary concern with the use of a developmental blanket material is its ability to form a strong, fatigue-resistant joint with solar cells. As noted above, the material selected produces a low CTE mismatch between cell and substrate which is a central contributor to thermal cycle fatigue capability. To demonstrate the applicability of the UltraFlex open weave material as a solar array blanket substrate, a small coupon (approx. 8 x 7 in.) was assembled with 10 large area (3.2 x 6.7 cm) silicon BSR cells of 7 mil thickness (Figure 6). The coupon was electrically tested and subjected to various thermal cycles. The test phases are given in Table 2.

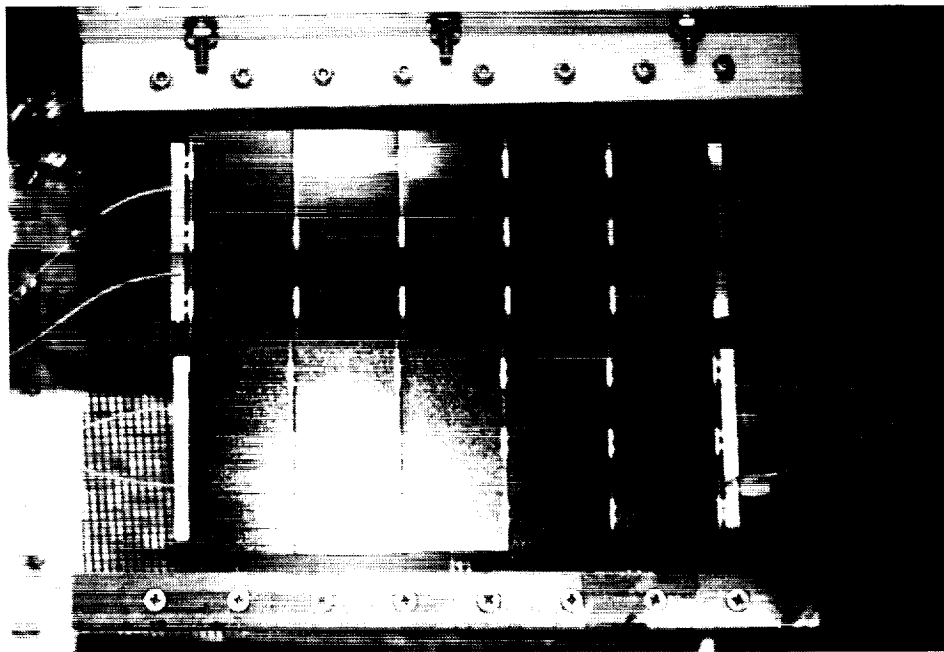


Figure 6  
UltraFlex Substrate Coupon

Table 2 Thermal Cycle Testing Parameters and Results			
Test Phase	Cold Temperature (°C)	Hot Temperature (°C)	Number of Cycles
1	+ 55	- 61	5808
2	+ 70	- 70	1004
3	+ 100	- 150	In Progress 4 Completed 50 Planned

Test results through phase 2 were quite successful with no cell-substrate delaminations, cracked cells or coverslides, or interconnect failures observed. The coupon was then electrically tested to ensure no electrical degradation had occurred. The electrical test data before and after thermal cycling is shown in Table 3. The degradation observed was within the limits of test error. The UltraFlex substrate thus demonstrated bondability, bond strength and the ability to survive environmental testing with negligible mechanical or electrical degradation. It is therefore an excellent candidate material for solar array blanket substrates.

Table 3 Thermal Cycling Cell Degradation			
	Pre-Test	Post-Test	Change (%)
ISC	0.818	0.811	-0.86
Voc	5.442	5.435	-0.13
Imp	0.771	0.767	-0.52
Vmp	4.523	4.515	-0.18

## ANALYTICAL PERFORMANCE

### Thermal Analysis

To estimate on-orbit solar array power production the cell operating temperature must be determined. For this purpose a one-dimensional thermal model was constructed. However, the rearside of the substrate is an open mesh with distinct two-dimensional properties. To maintain the simplicity of the one-dimensional model the substrate radiative properties were approximated with an exposed area weighting method (Figure 7).

$$\Phi_{a,cell} = (\Phi_{a, total}) (A_{cell}) (\alpha_{cell})$$

and

$$\Phi_{a,sub} = (\Phi_{a, total}) (A_{sub}) (\alpha_{sub})$$

- Where:
- $\Phi_{a, total}$  = Total albedo input flux.
  - $\Phi_{a,cell}$  = Cell albedo input flux.
  - $\Phi_{a,sub}$  = Substrate albedo input flux.
  - $A_{cell}$  = Cell rearside area ratio.
  - $A_{sub}$  = Substrate rearside area ratio.
  - $\alpha_{cell}$  = Cell rearside solar absorbtivity.
  - $\alpha_{sub}$  = Substrate rearside solar absorbtivity.

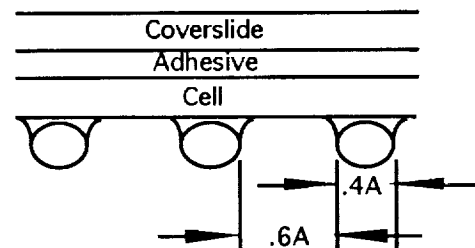


Figure 7  
One-Dimensional Thermal Model

A similar formulation was used for rearside earth infrared (IR) flux input but with IR absorptivities. The rearside cell emission was also approximated with the above technique but to account for the increased emissive area of the fabric mesh bundles, an additional area factor term was included.

$$\epsilon_{a,sub} = (\pi/2) (A_{sub}) (\epsilon_{sub})$$

Where:  $\pi/2$  = Area multiplier to account for 2-D shape of fabric emissive surface. (See Figure 7)  
 $\epsilon_{sub}$  = Cell rearside emissivity.

The thermal model was run and cell operational temperatures were collected for multiple orbits and seasons. The results are given in Table 4.

Table 4 Thermal Analysis Results								
Orbit	Silicon Cells				GaAs/Ge Cells			
	Low Earth		Geostationary		Low Earth		Geostationary	
	BOL	EOL	BOL	EOL	BOL	EOL	BOL	EOL
Equinox	77.6 °C	81.5 °C	50.0 °C	55.2 °C	85.9 °C	89.3 °C	60.4 °C	65.8 °C
Summer Solstice	67.4 °C	78.5 °C	38.8 °C	44.9 °C	75.3 °C	78.7 °C	50.2 °C	55.5 °C
Winter Solstice	72.2 °C	78.4 °C	44.2 °C	50.6 °C	80.1 °C	83.7 °C	55.8 °C	61.2 °C

### Power Analysis

On-orbit power production analyses were performed for the UltraFlex prototype wing currently under construction. The current prototype design specifies the use of 3960 2.4 mil BSFR cells (13.70%, 21.8 mg/cm<sup>2</sup>) with 4 mil CMX coverslides assembled into 99 cell strings. The analysis was also performed for an array based on 3.5 mil GaAs/Ge solar cells (18.33%, 55 mg/cm<sup>2</sup>) with 4 mil CMX coverslides. The analysis was done for both LEO (555 km, i=60°, 7-year) and GEO (10-year) applications. Two axis solar tracking was assumed. The resultant power predictions are presented in Table 5.

Table 5 Power Production Analysis Results								
Orbit	Silicon Cells				GaAs/Ge Cells			
	Low Earth		Geostationary		Low Earth		Geostationary	
	BOL	EOL	BOL	EOL	BOL	EOL	BOL	EOL
Equinox	778 W	645 W	888 W	660 W	1184 W	1011 W	1235 W	939 W
Summer Solstice	791 W	634 W	823 W	612 W	1166 W	996 W	1114 W	848 W
Winter Solstice	826 W	678 W	860 W	639 W	1237 W	1056 W	1181 W	898 W

### Mass Properties

A mass properties analysis was performed for the prototype unit based on volumetric calculations of piece part weights. The masses of the major contributors, the solar cells and the substrate, have been confirmed by test. A 5% contingency is also carried for conservatism. The mass breakdown is given in Table 6.



Table 6 Prototype Mass Breakdown		
Subassemblies	2.4 mil Silicon Version	3.5 mil GaAs/Ge Version
Substrates and Adhesives	546	546
Cells	3163	4982
Spars	282	282
Harnesses	101	101
Pivot Panel	350	350
Static Panel	285	285
Center Hub	90	90
Deploy Mechanism	217	217
Subtotal	5177	6996
Contingency (5%)	259	350
Total (grams)	5436	7346

The above results were combined with Table 5 to produce array specific power performance estimates. This data is given in Table 7 and again in Figure 8 as an overlay on the previous specific power efficiencies given in Figure 1.

Table 7 Specific Power Results								
Orbit	Silicon Cells				GaAs/Ge Cells			
	Low Earth		Geostationary		Low Earth		Geostationary	
	BOL	EOL	BOL	EOL	BOL	EOL	BOL	EOL
Equinox	143 W/kg	119 W/kg	163 W/kg	121 W/kg	161 W/kg	138 W/kg	168 W/kg	128 W/kg
Summer Solstice	145 W/kg	117 W/kg	151 W/kg	113 W/kg	159 W/kg	136 W/kg	152 W/kg	115 W/kg
Winter Solstice	152 W/kg	125 W/kg	158 W/kg	118 W/kg	168 W/kg	144 W/kg	161 W/kg	122 W/kg

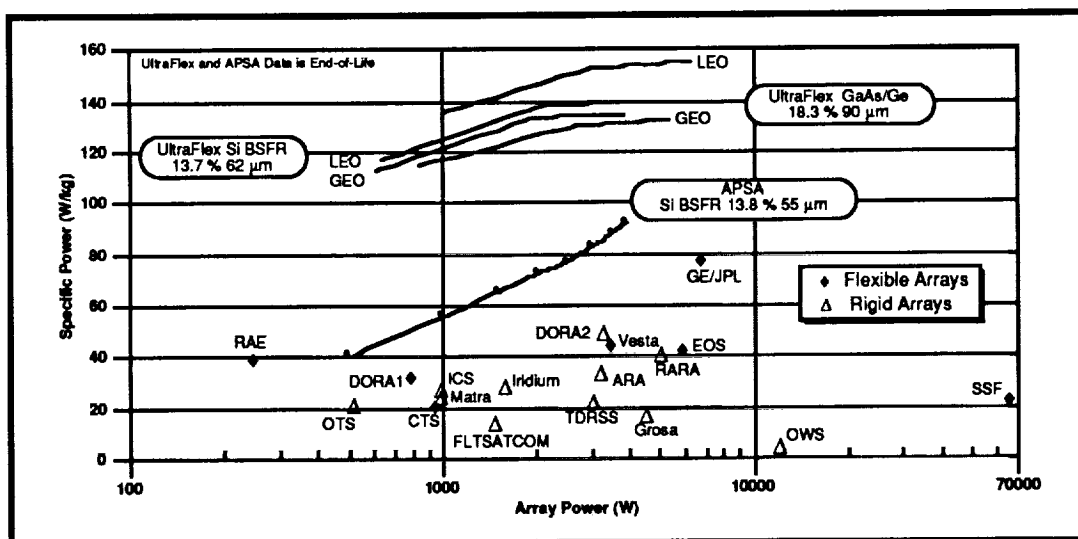


Figure 8  
UltraFlex End-of-Life Specific Power

## Deployed Structural Analysis

An ANSYS finite element model of the deployed UltraFlex array was developed to verify that the wing's performance fulfilled the structural requirements defined in Table 1. The stiffening effect of the prestressed gores and spars, which results from the pretensioned nature of the deployed system, needed to be accounted for in the analysis. The model consisted of shell elements that represented the tensioned gore sections and beam elements that represented the spars. The modeling approach employed material properties that were tailored such that a single gore section would have the same fundamental frequency (i.e., mass and stiffness matrix terms) as would a similar model of that was pretensioned by directly applied in-plane circumferential loads. With this technique successive loading steps were avoided. The array "cupping" was introduced directly into the model geometry. This modeling approach gave reasonable results for deployed acceleration and frequency calculations.

Using this model, a modal analysis was performed to determine the frequencies and mode shapes of the deployed UltraFlex array. The first fundamental mode for the prototype array design is a torsional motion of the gore sections about the support panel axis, as shown in Figure 9. A parametric study was then performed to assess the effect of gore tension variations (and corresponding "cup" deflections) on deployed frequencies. Preliminary results of this analysis indicate that the frequency will increase in an approximately linear fashion as gore tension is increased up to about 0.10 lb/in after which the frequency changes are minimal. Since the baseline pretensions are in excess of 0.10 lb/in, slight preload variations due to tolerance build-ups or thermally induced deflections will have minimal effects on the deployed characteristics.

The deployed model was subjected to accelerations about each of the orthogonal array axes to determine maximum allowable acceleration loads. The critical limiting load is an out-of-plane acceleration of 0.4 g's, which causes the gore to "snap through" to an equilibrium state where the gore is cupped in the other direction. This "snap-through," while not advised, is not considered to be catastrophic to the operation of the array.

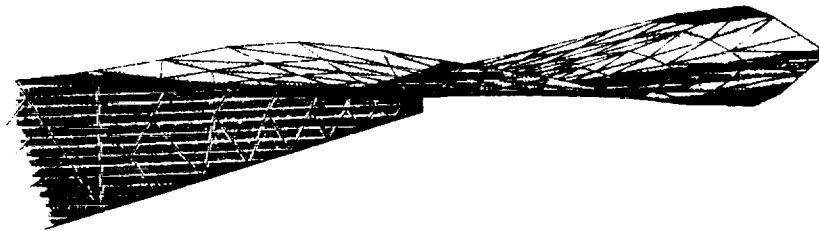


Figure 9  
Deployed Minimum Mode Frequency

---

## CONCLUSION

The UltraFlex solar array design has been presented as a viable advanced photovoltaic candidate for consideration as a power source for near or far term spacecraft. Any of the UltraFlex's superior performance characteristics, extremely low array mass, low deployed inertia, reduced center-of-pressure offset, or intrinsic damping capability, can potentially be mission enabling.

The underlying tenant of the UltraFlex concept is the use of superior performance to reduce program costs. As noted above program cost savings can be realized many ways. With today's launch costs averaging around [5] \$7,302 per pound, for a LEO, and about \$54,307 per pound for a GEO insertion, a two kilowatt UltraFlex wing's low mass can save about 685 k\$ and 5,251 k\$, respectively. However, in a more realistic scenario, a launch vehicle will be selected and funded for a given mission and, in due course, the vehicle's payload will be fully allocated. In this case, the solar array weight savings will be reallocated for additional payloads such as experiments, communication transponders, or maneuvering fuel in an effort to maximize mission "payoff." This payoff will be realized as additional scientific data or additional operational capability. In some extreme cases the weight savings afforded by the use of the UltraFlex array will allow use of a smaller class of launch vehicle. The step-wise cost savings realized

in this situation can be significant. There may also be some cases where the reduced spacecraft mass does not allow a down-scaled launcher but does allow the spacecraft to be inserted into an orbit which may be more desirable. Additionally, the reduced UltraFlex inertia will require less station-keeping fuel to stabilize over the course of a mission. The unneeded fuel may be used for a longer mission life or its mass may be used for additional payload.

To date significant design, analytical, and material studies have been performed by the ABLE/Spectrolab team and a prototype model is currently under construction. A qualification test unit is currently planned with testing to be completed in late 1993. Upon initial examination the concept satisfies the standard criteria for spacecraft solar array systems. These include superior specific power performance, small stowed volume requirement, high reliability, sufficient structural and environmental capability, and an established technology basis.

---

## REFERENCES

1. Solar Cell Array Design Handbook Volume 1 and 2, JPL Publication No. SP 43-48, October 1986.
  2. *Retractable Advanced Rigid Array*, DeKam, 1988, IEEE.
  3. *Advanced Photovoltaic Solar Array Prototype Development and Testing, Final Review Data Package, Phase III*, NASA JPL Contract 957990, 12 August 1991.
  4. The Advanced Photovoltaic Solar Array Program, R. Kurland, P.M. Stella, ESA SP-294, August 1989.
  5. NASA. Pentagon Chart Ambitious Unmanned Launch Vehicle Program, E.H. Kolcum, Aviation Week and Space Technology, Vol. 136, No. 11, March 16, 1992.
-